INT. J. CONTROL, 2004, VOL. 77, NO. 13, 1189–1199

Taylor & Francis
Taylor & Francis Group

# Multi-channel learning using anticipatory ILCs

DANWEI WANG†* and YONGQIANG YE†

In general, a linear system with a single iterative learning controller (ILC) has a limited learnable frequency bandwidth. This limitation affects learning transient and final tracking accuracy. In this paper, a *multi-channel* method is proposed to extend the learning frequency bandwidth beyong that achievable by a single ILC. Each channel requires a single learning controller designed to fit the system dyanmics within this designated frequency band. To prepare tracking errors for each channel, DFT/IDFT and zero-phase filters are used. Learning using anticipatory learning control under the multi-channel structure is analysed in detail. The design procedure and effectiveness of the multi-channel method are demonstrated via simulations and experiments. Comparison of the multi-channel learning control with the conventional single-channel learning control highlights the merits of the multi-channel design method.

## 1. Introduction

The concept of iterative learning control (ILC) was proposed by Arimoto *et al.* (1984) to improve tracking of robot trajectories. Learning control aims to reduce tracking error during the whole period of a process operation including the transient part using minimum knowledge of the system. This is accomplished by using the past experience with the same task to improve the performance in the future operations.

Since its emergence, ILC has received considerable attention. Most existing works focus on the convergence issues. In applications, mathematically proved convergence conditions cannot guarantee reasonable transients during the learning process (Longman 2000). Therefore, in recent years, increasing efforts have been made on the design issues (Amann *et al.* 1996, Phan and Juang 1996, Doh *et al.* 1998, Moon *et al.* 1998, Longman 2000, Chen and Moore 2001, Tan *et al.* 2001). In most approaches, the input update is acquired directly from the error information of the previous repetition(s). Usually the learning control has only one learning compensator. An alternative approach is to treat harmonic components of the tracking error individually. The frequency coefficients of the input update is firstly derived from the discrete fourier transform (DFT) of the previous error, then the input update is achieved via inverse discrete fourier transform (IDFT) (Manabe and Miyazaki 1991, Lee *et al.* 1993, Huang and Cai 2000). If $n$ harmonic components are considered, the learning control has $n$ learning compensators in the frequency domain. The *multi-channel* design method proposed in this paper has a few (generally much less than the number of harmonic components) learning compensators working simultaneously, and the input update still takes place in the time domain.

Received 1 October 2003. Revised and accepted 5 August 2004.

*Author for correspondence. e-mail: edwwang@ntu.edu.sg

†School of Electrical and Electronic Engineering, Nanyang Technological University, Singapore 639798.

## 2. Single ILC and learnable Bandwidth

Consider a linear SISO system modelled by the transfer function

$$G_p(s) = \frac{Y(s)}{U(s)}. \tag{1}$$

The tracking error of the $j$th repetition is $E_j(s) = Y_d(s) - Y_j(s)$, where $Y_d(s)$ is the Laplace transform of a desired output $y_d(t)$ defined on a finite time operation interval $[0, T]$. Let the Laplace transform of a single learning law be

$$U_j(s) = U_{j-1}(s) + k\Phi(s)E_{j-1}(s) \tag{2}$$

where $k$ is the scalar learning gain and $\Phi(s)$, with DC gain of 1, is the learning compensator in Laplace form. Using (1) and (2) we get

$$\begin{aligned} Y_j(s) - Y_{j-1}(s) &= G_p(s)[U_j(s) - U_{j-1}(s)] \\ &= kG_p(s)\Phi(s)E_{j-1}(s). \end{aligned}$$

Since

$$Y_j(s) - Y_{j-1}(s) = -[E_j(s) - E_{j-1}(s)]$$

we get

$$E_j(s) = [1 - kG_p(s)\Phi(s)]E_{j-1}(s). \tag{3}$$

$[1 - kG_p(s)\Phi(s)]$ can be viewed as a transfer function from the tracking error at repetition $(j-1)$ to the tracking error at repetition $j$. Similar to Hideg and Judd (1988), Goh (1994), Longman (2000) and Chen and Moore (2001), the condition for the tracking error to

*International Journal of Control* ISSN 0020–7179 print/ISSN 1366–5820 online © 2004 Taylor & Francis Ltd
http://www.tandf.co.uk/journals
DOI: 10.1080/00207170412331297966

converge for all frequencies is

$$\left|1 - kG_p(j\omega)\Phi(j\omega)\right| < 1. \tag{4}$$

Frequency domain convergence condition is a sufficient condition for convergence though learning control is a finite time problem (Amann *et al.* 1996, Longman 2000). In general, the convergence condition (4) cannot be satisfied for all frequencies. The finite frequency range where (4) holds is termed *learnable frequency band (range)*. A cutoff is required to stop learning the error components with frequencies outside this learnable frequency band to prevent the divergence in learning as operation cycles increase.

## 3. Multi-channel approach

### 3.1. *Multi-channel ILC structure*

If the learnable frequency band of single learning controller is not wide enough, methods to extend the learnable frequency band are desirable. Longman and Wirkander (1998) and Wirkander and Longman (1999) use the self-tuning method, switching the parameters of learning compensator between repetitions and finding the best switch mode. The switching results in a much higher cutoff frequency (Wirkander and Longman 1999). Longman and Wirkander's idea can be generalized into switching the learning compensators, not just switching parameters. If we use learning compensator $\Phi_1(s)$ with learning gain $k_1$ for $\alpha$ trials, then switch to $\Phi_2(s)$ with learning gain $k_2$ for $\beta$ trials, then repeat, the total error contraction rate is

$$\left|1 - k_1 G_p(j\omega)\Phi_1(j\omega)\right|^{\alpha}\left|1 - k_2 G_p(j\omega)\Phi_2(j\omega)\right|^{\beta}.$$

It is possible to find an optimal ratio of $\alpha/\beta$ that will keep the total error contraction rate less than one up to a highest frequency. And this frequency will be higher than the cut-off frequency of using $\Phi_1(s)$ with $k_1$ or $\Phi_2(s)$ with $k_2$ alone.

The multi-channel method proposed here uses more than one learning compensators in parallel to cover a wider frequency band, but no switching is required. An ILC structure with $n$ channels is proposed in figure 1. The filter $F_i(s)$ defines the designated frequency band of the $i$th channel, $k_i$ is a scalar learning gain for the $i$th channel, and the $i$th learning compensator $\Phi_i(s)$ ensures the convergence of tracking error with the defined frequencies. The tracking error is separated into $n$ parts corresponding to the designated bands/channels. These separated error parts are learned simultaneously in corresponding channels. The individual learning control laws in the individual channels are

$$\left.\begin{aligned} U_{1,j}(s) &= U_{1,j-1}(s) + k_1\Phi_1(s)F_1(s)E_{j-1}(s) \\ &\text{in Channel 1} \\ &\vdots \\ U_{i,j}(s) &= U_{i,j-1}(s) + k_i\Phi_i(s)F_i(s)E_{j-1}(s) \\ &\text{in Channel } i \\ &\vdots \\ U_{n,j}(s) &= U_{n,j-1}(s) + k_n\Phi_n(s)F_n(s)E_{j-1}(s) \\ &\text{in Channel } n \end{aligned}\right\} \tag{5}$$

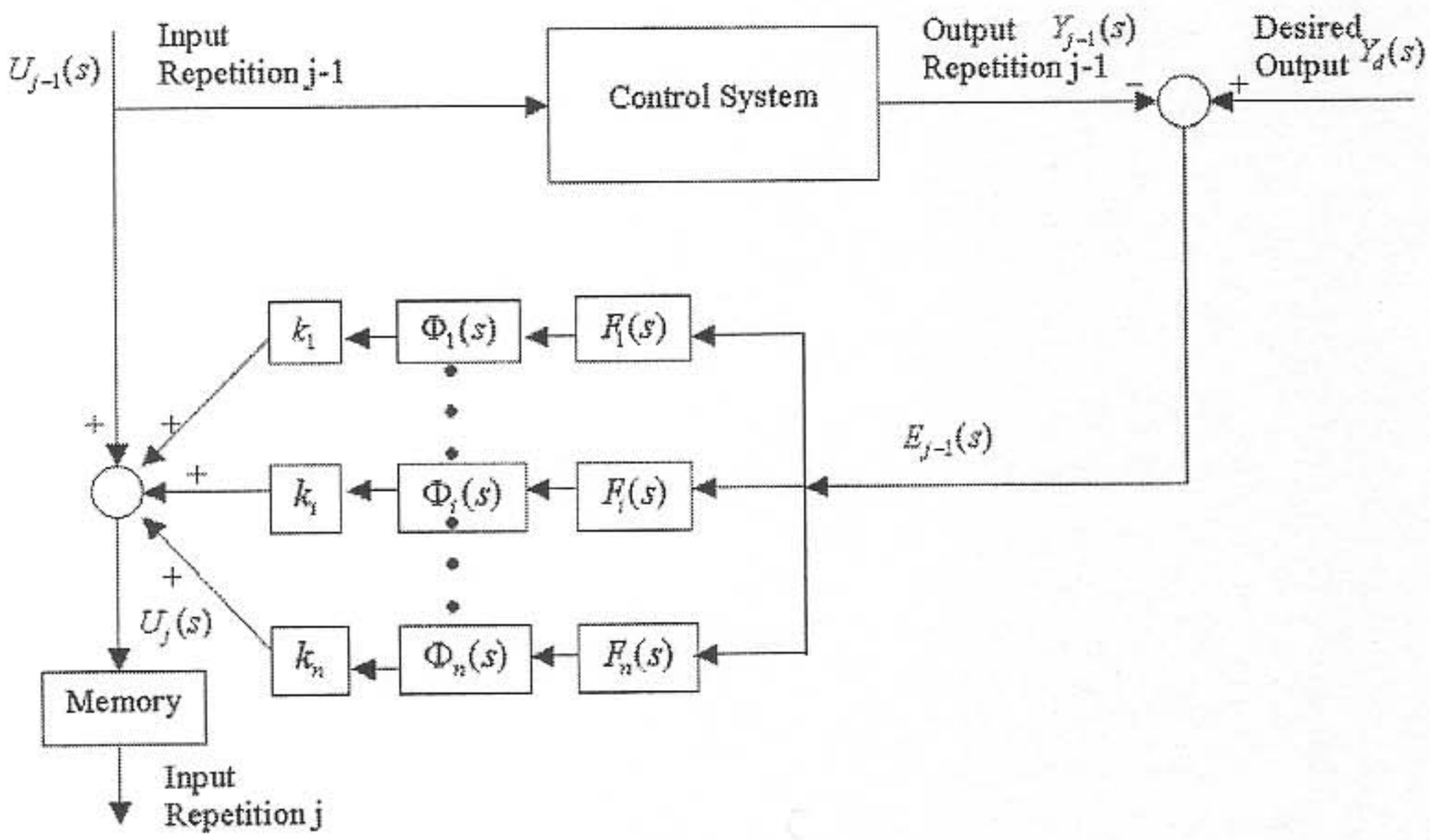


Figure 1. Multi-channel learning control.

The overall learning law is

$$\begin{aligned} U_j(s) &= \sum_{i=1}^{n} U_{i,j}(s) \\ &= \sum_{i=1}^{n} U_{i,j-1}(s) + \left(\sum_{i=1}^{n} k_i \Phi_i(s) F_i(s)\right) E_{j-1}(s) \qquad (6) \\ &= U_{j-1}(s) + \left(\sum_{i=1}^{n} k_i \Phi_i(s) F_i(s)\right) E_{j-1}(s). \end{aligned}$$

Using (4) and (6), the error contraction condition for multi-channels learning control is

$$\left|1 - G_p(j\omega) \sum_{i=1}^{n} k_i \Phi_i(j\omega) F_i(j\omega)\right| < 1. \qquad (7)$$

The time domain version of (5) and (6) are

$$u_j(t) = \sum_{i=1}^{n} u_{i,j}(t) \qquad (8)$$

with

$$\left.\begin{aligned} u_{1,j}(t) &= u_{1,j-1}(t) + k_1 L_1(e_{1,j-1}(t)) \\ &\quad \text{in Channel 1} \\ &\vdots \\ u_{i,j}(t) &= u_{i,j-1}(t) + k_i L_i(e_{i,j-1}(t)) \\ &\quad \text{in Channel } i \\ &\vdots \\ u_{n,j}(t) &= u_{n,j-1}(t) + k_n L_n(e_{n,j-1}(t)) \\ &\quad \text{in Channel } n \end{aligned}\right\} \qquad (9)$$

where $L_i(\cdot)$ is channel $i$'s learning algorithm corresponding to $\Phi_i(s)$ and $e_{i,j-1}(t)$ is the result of passing error at repetition $j-1$, $e_{j-1}(t)$, through filter $F_i(s)$. It should be noted that the input update of the multi-channel learning control still takes place in time domain which is different from the approaches in Manabe and Miyazaki (1991), Lee *et al.* (1993) and Huang and Cai (2000). The total input update is the sum of multiple learning control update. In the time domain, Tayebi and Zaremba (2002) proposed a gain-scheduling-based iterative learning controllers for continuous-time nonlinear systems described by a blended multiple model representation. In Tayebi and Zaremba (2002), the learning gain changes according to the values of the validity functions depending on the operating point in the time domain, while in our approach, the learning compensator or parameter depends on frequency. The idea of using summational multiple functions to represent a blended model is similar to our multi-channel method. In the time domain, no non-split input update (single learning controller) can realize the blended learning compensator in multi-channel learning control. Only split input update (multiple learning controllers) can.

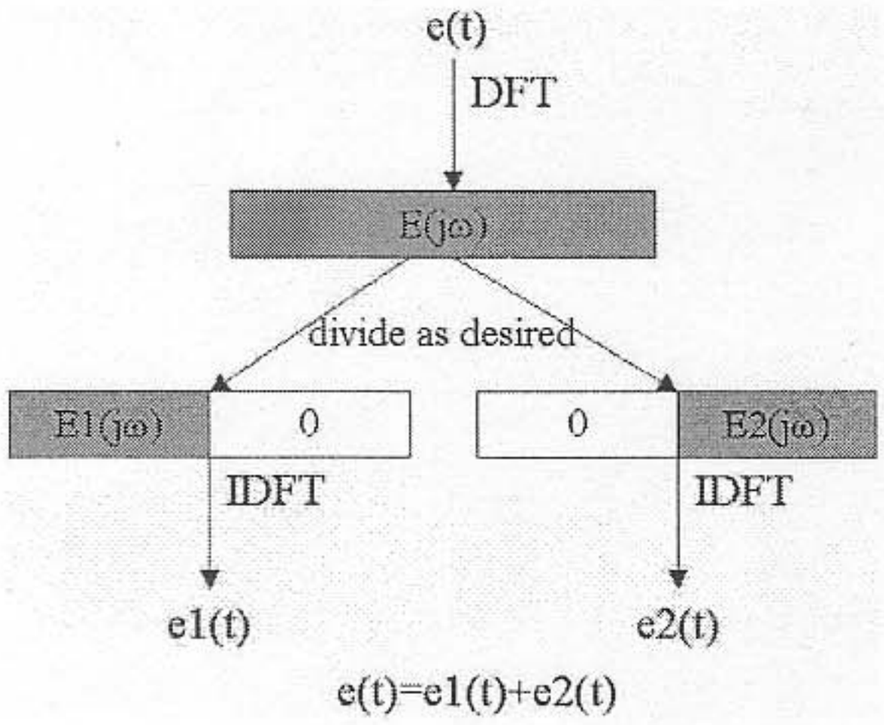


Figure 2. Error separation via DFT/IDFT.

### 3.2. *Error separation*

The channel filters, $F_i(s)$ in figure 1, can be realized with a discrete Fourier transform/inverse discrete Fourier transform (DFT/IDFT) pair or zero-phase filter.

3.2.1. *DFT/IDFT approach.* Though $F_i(s)$ is considered as continuous, any numerical implementation should use sampled-data. DFT/IDFT and zero-phase filter have been used in cutoff in ILC (Longman and Songchon 1999, Plotnik and Longman 1999). Technical details addressing DFT/IDFT and zero-phase filters are reported in Plotnik and Longman (1999). Figure 2 demonstrates the error separation into two parts according to two designated frequency bands/channels. First, using DFT, the error frequency spectrum $E(j\omega)$ can be obtained from the error signal $e(t)$. Second, the frequency spectrum $E(j\omega)$ is divided into two designated bands/channels. Third, the rest of each of the two segments is padded with zero. At last, using IDFT, two error sequences, $e1(t)$ and $e2(t)$, can be obtained from the two bands of spectrum. This way, the original error signal is separated into two error signals with different frequency spectrums, i.e., $e(t) = e1(t) + e2(t)$.

3.2.2. *Zero-phase filter approach.* A zero-phase filter is not a perfect cutoff device, but rather attenuates the signals above/below the cutoff frequency at a rate determined by the order of the filter. Therefore, two adjacent zero-phase filters will produce an overlapping frequency region between the two designated frequency bands/channels. Figure 3 demonstrates the partial overlapping between lowpass Filter 1 and highpass Filter 2. $\omega_{c1}$ and $\omega_{c2}$ are the passband edge frequencies (i.e., cutoff frequencies) of Filter 1 and

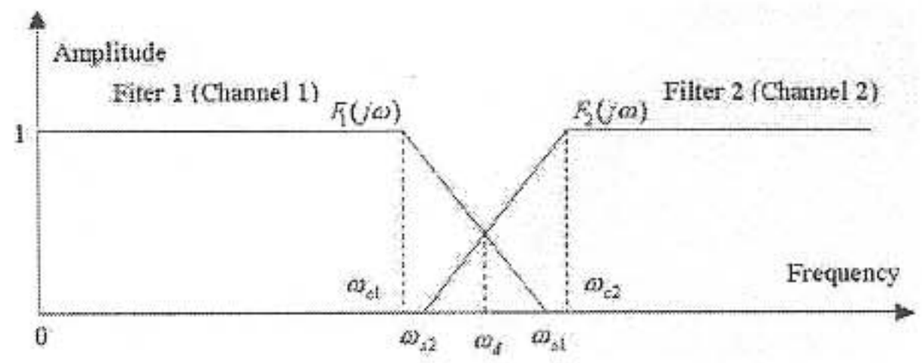


Figure 3. Overlapping of two filters.

Filter 2, respectively; $\omega_{s1}$ and $\omega_{s2}$ are the stopband edge frequencies of Filter 1 and Filter 2, respectively (Les 1996). Note that $\omega_{c1} < \omega_{c2}$ and $\omega_{s2} < \omega_{s1}$. Suppose the overlapping region is $\delta\omega = \omega_{s1} - \omega_{s2}$ and $\omega_d$ is the desired separation point of the two designated frequency bands for channels 1 and 2. The equivalent learning compensator inside the region $\delta\omega$, in Laplace form, will be

$$k_1\Phi_1(s)F_1(s) + k_2\Phi_2(s)F_2(s)$$

where $k_1/\Phi_1(s)$ and $k_2/\Phi_2(s)$ are the two learning gains/compensators of channels 1 and 2, respectively; $F_1(s)$ and $F_2(s)$ are the two designated zero-phase filters that define the frequency bands in channels 1 and 2, respectively. Because zero-phase filters generate no phase shift, $F_1(s)$ and $F_2(s)$ are real, positive value functions. Inside the overlapping region, we have $0 < F_1(j\omega) < 1$ and $0 < F_2(j\omega) < 1$, and both learning compensators are stable, i.e.

$$\left.\begin{aligned} |1 - k_1 G_p(j\omega)\Phi_1(j\omega)| \le 1 \\ |1 - k_2 G_p(j\omega)\Phi_2(j\omega)| \le 1 \end{aligned}\right\} \tag{10}$$

Note that the two '=' in (10) should not happen at the same frequency. Then the error contraction rate in the overlapping region $\delta\omega$ is

$$\begin{aligned} &|1 - G_p(j\omega)(k_1\Phi_1(j\omega)F_1(j\omega) + k_2\Phi_2(j\omega)F_2(j\omega))| \\ &= 1(1 - k_1 G_p(j\omega)\Phi_1(j\omega))F_1(j\omega) \\ &\quad + (1 - k_2 G_p(j\omega)\Phi_2(j\omega))F_2(j\omega) + 1 - F_1(j\omega) - F_2(j\omega)| \\ &\le |1 - k_1 G_p(j\omega)\Phi_1(j\omega)|F_1(j\omega) \\ &\quad + |1 - k_2 G_p(j\omega)\Phi_2(j\omega)|F_2(j\omega) + |1 - F_1(j\omega) - F_2(j\omega)| \\ &< F_1(j\omega) + F_2(j\omega) + |1 - F_1(j\omega) - F_2(j\omega)|. \end{aligned}$$

If, inside the overlapping region

$$F_1(j\omega) + F_2(j\omega) \le 1 \tag{11}$$

then

$$F_1(j\omega) + F_2(j\omega) + |1 - F_1(j\omega) - F_2(j\omega)| = 1.$$

Thus we have

$$|1 - G_p(j\omega)(k_1\Phi_1(j\omega)F_1(j\omega) + k_2\Phi_2(j\omega)F_2(j\omega))| < 1.$$

Therefore (10) and (11) are the design requirements for the zero-phase filters and learning compensators and these requirements will sufficiently guarantee the error contraction in the overlapping region.

## 4. Learning with multiple anticipatory ILCs

The linear anticipatory ILC law (Wang 2000) has the simple form of

$$u_j(t) = u_{j-1}(t) + ke_{j-1}(t + \Delta) \tag{12}$$

where $k$ is the learning gain and $\Delta$ is the lead-time. The error contraction condition (4) for the anticipatory ILC is

$$|1 - k\, e^{j\Delta\omega} G_p(j\omega)| < 1. \tag{13}$$

Suppose $G_p(j\omega) = N_p(\omega)\exp(j\theta_p(\omega))$ with $N_p(\omega)$ being the magnitude characteristics, and $\theta_p(\omega)$ being the phase characteristics of the system, respectively. From (13), we get

$$\left|1 - kN_p(\omega)\, e^{j(\theta_p(\omega)+\Delta\omega)}\right| < 1. \tag{14}$$

If $k > 0$, we have

$$kN_p(\omega) < 2\cos(\theta_p(\omega) + \Delta\omega). \tag{15}$$

The frequency range where condition (15) is satisfied is termed *causal range*.

For a minimum phase process

$$G_p(s) = \frac{b_m s^m + b_{m-1}s^{m-1} + \cdots + b_1 s + b_0}{s^n + a_{n-1}s^{n-1} + \cdots + a_1 s + a_0}$$

with more poles than zeros ($n > m$), the phase characteristic is approaching $-(n - m) \times 90°$. $\theta_p(\omega)$ is bounded while $\Delta\omega$ is approaching $+\infty$. In general, one single anticipatory ILC has one constant lead-time and satisfies (15) for a limited frequency band. Using the multi-channels method, we can have the learning law

$$u_j(t) = \sum_{i=1}^{n} u_{i,j}(t) \tag{16}$$

with

$$\left.\begin{aligned} u_{1,j}(t) &= u_{1,j-1}(t) + k_1 e_{1,j-1}(t + \Delta_1) && \text{in Channel 1} \\ &\vdots \\ u_{i,j}(t) &= u_{i,j-1}(t) + k_i e_{i,j-1}(t + \Delta_i) && \text{in Channel } i \\ &\vdots \\ u_{n,j}(t) &= u_{n,j-1}(t) + k_n e_{n,j-1}(t + \Delta_n) && \text{in Channel } n \end{aligned}\right\} \tag{17}$$

where $e_{i,j-1}$ is the $i$th error part corresponding to channel $i$ at repetition $j-1$. Condition (15) is satisfied

in all designated frequency bands/channels with some properly chosen learning gain $k_i$ and lead-time $\Delta_i$,

$$\left\{\begin{array}{ll} k_1 N_p(\omega) < 2\cos(\theta_p(\omega) + \Delta_1\omega) & \text{in Channel 1} \\ \vdots & \\ k_i N_p(\omega) < 2\cos(\theta_p(\omega) + \Delta_i\omega) & \text{in Channel } i \\ \vdots & \\ k_n N_p(\omega) < 2\cos(\theta_p(\omega) + \Delta_n\omega) & \text{in Channel } n \end{array}\right\} \quad (18)$$

Thus all error components within any of the designated frequency bands/channels will converge to zero. Unlike the self tuning method (Longman and Wirkander 1998, Wirkander and Longman 1999) which uses a repetition switching lead-steps (lead-time), multi-channels method fixes a lead-time of an anticipatory learning control for each of the designated frequency bands/channels.

## 5. An illustrative example and simulations

Consider the robot joint example used in Longman and Songchon (1999)

$$G_p(s) = \frac{8.8}{s+8.8}\,\frac{37^2}{s^2 + 2\times 0.5\times 37 s + 37^2}$$

Suppose a desired trajectory is given as, for $t \in [0, 1]$ s

$$y_d(t) = 1 - \cos 2\pi t + 0.3(1 - \cos 8\pi t) + 0.2(1 - \cos 38\pi t) + 0.1(1 - \cos 50\pi t)$$

and it contains frequency components of 1, 4, 19 and 25 Hz. The integration step size is 0.01 s. Learning gain $k$ is fixed as 1 (the reciprocal of DC gain of $G_p(s)$ — the maximum reasonable value suggested by Longman (2000)) in the simulations, i.e. in single-channel learning, $k$ is 1 and in multi-channel learning, $k$ is also 1 for all channels. The input of the first trial is $u_0(t) = 0$.

To ensure the error convergence of all frequency components, the learning control needs to be adjusted so that condition (15) is satisfied in a frequency band wider than [0, 25] Hz. In single-channel learning, we test a few values of the lead-time $\Delta$ (i.e. tune the lead-time $\Delta$) and try to find a value that can satisfy condition (15) in a widest frequency range (we plot (15) vs. frequency with different lead-times and find the one that offers the highest cutoff frequency). The final chosen value of lead-time is $\Delta = 0.05$ s and it yields a learnable frequency range [0, 18.7] Hz. Unfortunately, the components with frequencies 19 and 25 Hz is not covered and thus a multi-channel learning control is deployed to extend the maximum learnable frequency from 18.7 Hz to above 25 Hz. The $\Delta$ chosen above in the single-channel A-type learning control can be used in channel 1 and renamed as $\Delta_1$, with values $\Delta_1 = 0.05$ s. To ensure learning of all frequency components, channel 2 must have a designated frequency band to well cover [18, 25] Hz. Lead-time $\Delta_2 = 0.03$ s is chosen and the final design result is shown in figure 4. $\Delta_2$ has two causal ranges, [0, 4] Hz and [13.6, 32] Hz. The second causal range, [13.6, 32] Hz, of $\Delta_2$ overlaps with the

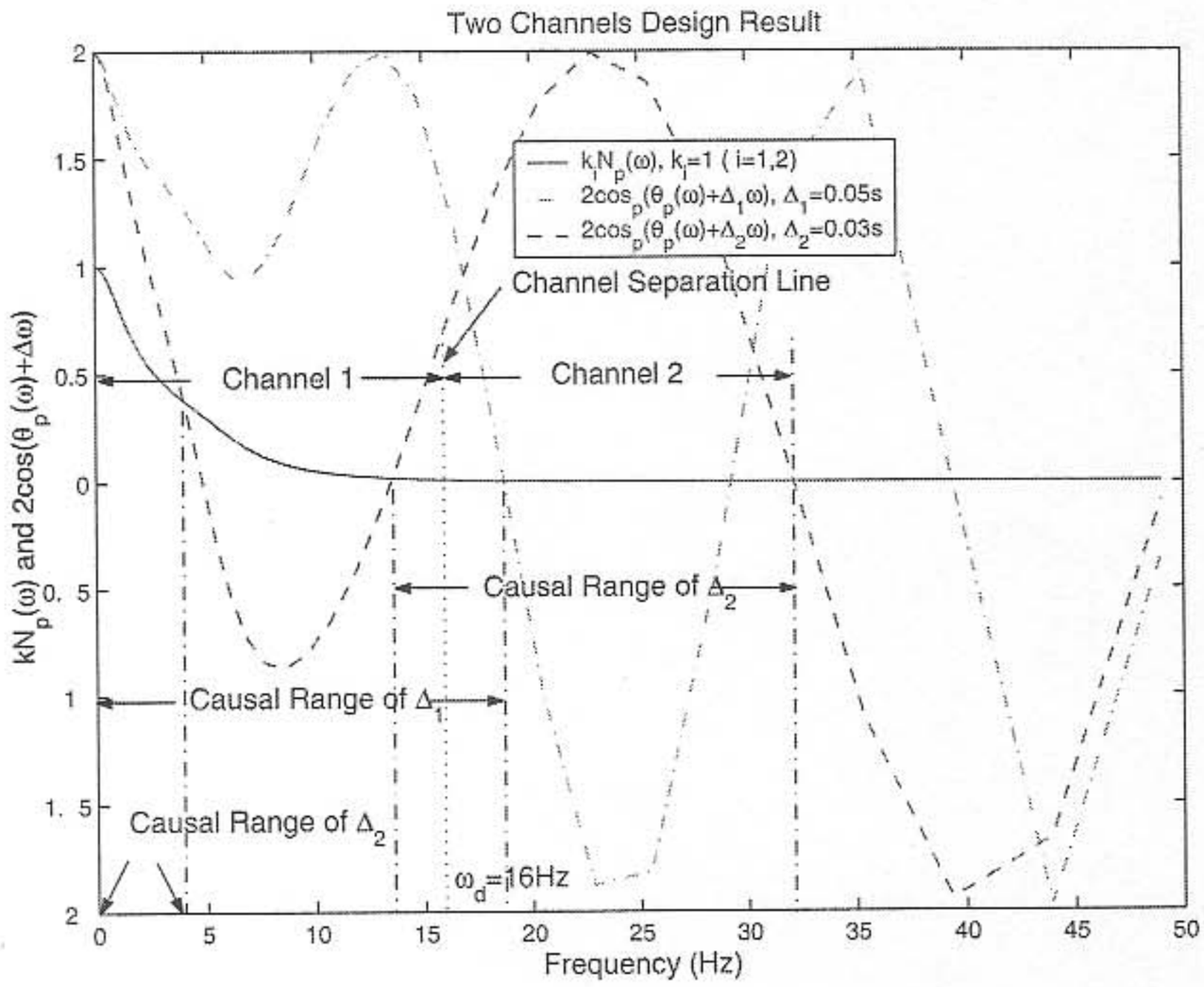


Figure 4. Two channels design result.

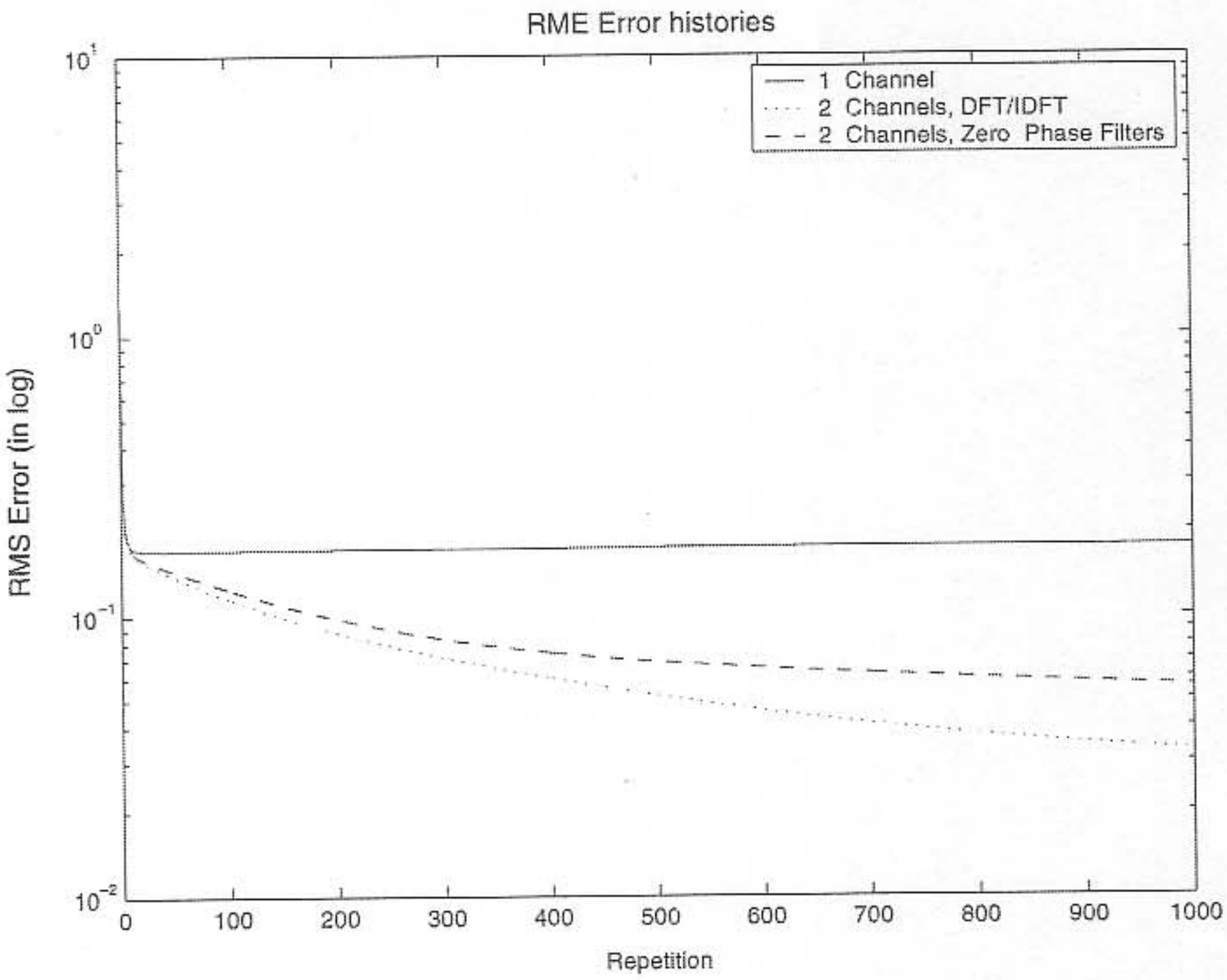


Figure 5. RMS error histories.

causal range, [0, 18.7] Hz, of $\Delta_1$. We can divide [0, 32] Hz into the following two designated bands,

$$\left.\begin{array}{l}\text{Channel 1 } (0\,\text{Hz} \le f < 16\,\text{Hz}) \quad \text{associated with } \Delta_1 \\ \text{Channel 2 } (16\,Hz \le f < 32\,Hz) \quad \text{associated with } \Delta_2\end{array}\right\}$$

The channel separation frequency point $\omega_d$, 16 Hz, locates in the middle of [13.6, 18.7] Hz to provide some robustness against model inaccuracy. When using zero-phase filters to separate the error, the overlapping region of two adjacent filters should locate inside [13.6, 18.7] Hz for the reason of (10) and (11). Then the multi-channel learning law is

$$u_j(t) = u_{1,j}(t) + u_{2,j}(t)$$

with

$$\left.\begin{array}{ll}u_{1,j}(t) = u_{1,j-1}(t) + e_{1,j-1}(t+0.05) & \text{in Channel 1} \\ u_{2,j}(t) = u_{2,j-1}(t) + e_{2,j-1}(t+0.03) & \text{in Channel 2}\end{array}\right\}$$

In single-channel learning, lead-time 0.05 s is used and the cutoff frequency is set as 18 Hz (realized by DFT/IDFT). In multi-channels learning, the cutoff frequency is set as 31 Hz. Two error separation approaches, DFT/IDFT approach and zero-phase filter approach are both tested. The RMS error histories for multi-channel learning and single-channel learning are shown in figure 5. In the single-channel case, the RMS error stops decreasing after about 50 repetitions. Tracking performances of single-channel learning and multi-channel learning at repetition 1000 are shown in figure 6. It is obvious that the multi-channel learning tracks the desired trajectory more accurately than the single-channel learning.

## 6 Experiments

Experiments are performed using joint 3 of an industrial robot, SEIKO TT3000, which is a SCARA type robotic manipulator as shown in Figure 7. Joint 3 controls one link moving in a horizontal plane and the closed-loop transfer function of joint 3 can be approximated as

$$G_p(s) = \frac{948}{s^2 + 42s + 948}.$$

The desired position trajectory is a smooth cycloid plus two prominent high frequency terms

$$y_d(t) = \sum_{n=1}^{51} a_n[1 - \cos(\omega_n t)] + 0.05[1 - \cos(80\pi t)] + 0.03[1 - \cos(90\pi t)]\text{degree};$$
$$0 \le t \le 10\,\text{s} \tag{19}$$

where $\omega_n$ are $0.1\pi$, $2\pi$, $4\pi$, $6\pi$, ..., $100\pi$, and $a_n = 80\,e^{-\omega_n}$, noting that the two prominent high frequencies are 40 and 45 Hz. Learning gain $k$ is fixed as 0.5 in the experiments, i.e. in single-channel learning,

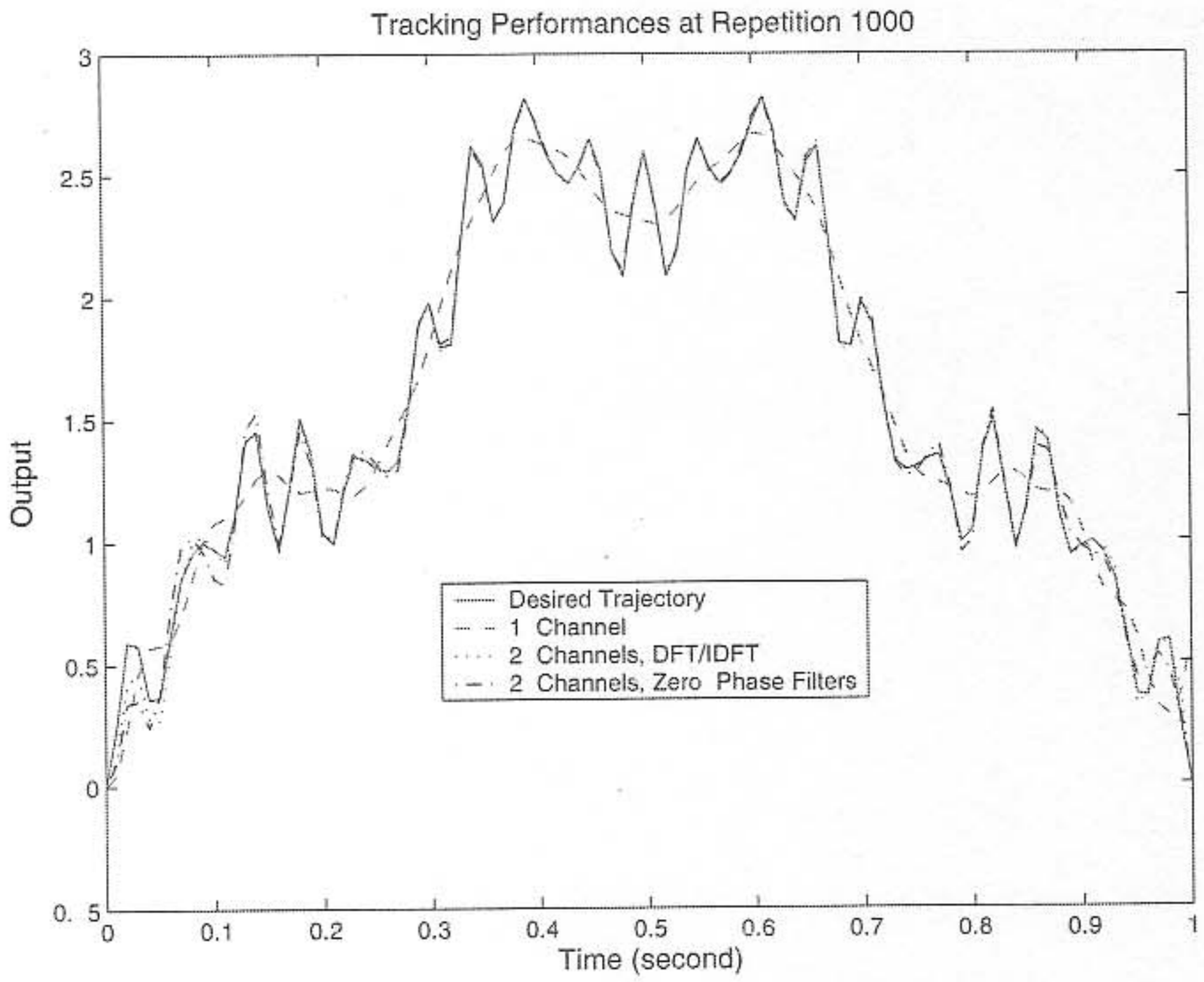


Figure 6. Tracking performances.

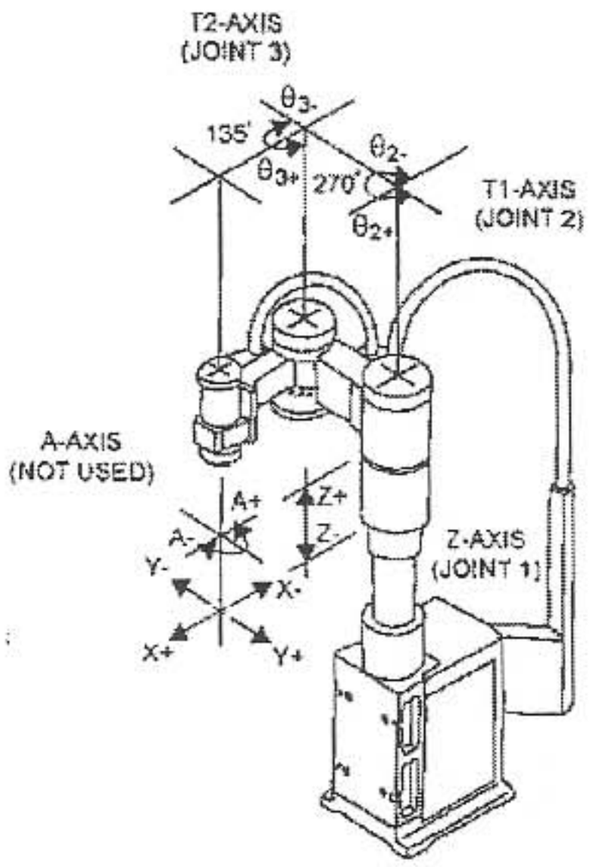


Figure 7. Experimental robot arm.

$k$ is 0.5 and in multi-channel learning, $k$ is also 0.5 for all channels. The initial input is again $u_0(t) = 0$.

Similar design procedure is carried out as that in §5 and details can be found in Ye and Wang (2002). The final design result is shown in figure 8. Because the sampling frequency is at 100 Hz, the learnable frequency band should be no more than 50 Hz, half of the sampling frequency. [0, 50] Hz is divided into the following two designated bands

$$\left.\begin{array}{r}\text{Channel 1}(0\,\text{Hz} \le f < 31\,\text{Hz}) \\ \text{associated with } \Delta_1 = 0.02\,\text{s} \\ \text{Channel 2}(31\,\text{Hz} \le f \le 50\,\text{Hz}) \\ \text{associated with } \Delta_2 = 0.01\,\text{s}\end{array}\right\}.$$

$\Delta_2$ has two causal ranges, [0, 4] Hz and [20, 50] Hz. The second causal range, [20, 50] Hz, of $\Delta_2$ overlaps with the causal range, [0, 36] Hz, of $\Delta_1$. The channel separation frequency point $\omega_d = 31$ Hz locates in the middle of [20, 36] Hz to provide some robustness against model inaccuracy. Then the multi-channels learning law is

$$u_j(t) = u_{1,j}(t) + u_{2,j}(t)$$

with

$$\left.\begin{array}{rcl} u_{1,j}(t) &=& u_{1,j-1}(t) + 0.5e_{1,j-1}(t+0.02) \\ & & \text{in Channel 1} \\ u_{2,j}(t) &=& u_{2,j-1}(t) + 0.5e_{2,j-1}(t+0.01) \\ & & \text{in Channel 2}\end{array}\right\}$$

In multi-channel learning, no cutoff is employed, so the learnable frequency range of the multi-channel learning control is [0, 50] Hz. Two error separation approaches, the DFT/IDFT approach and the zero-phase filters approach are both tested. For the zero-phase filters

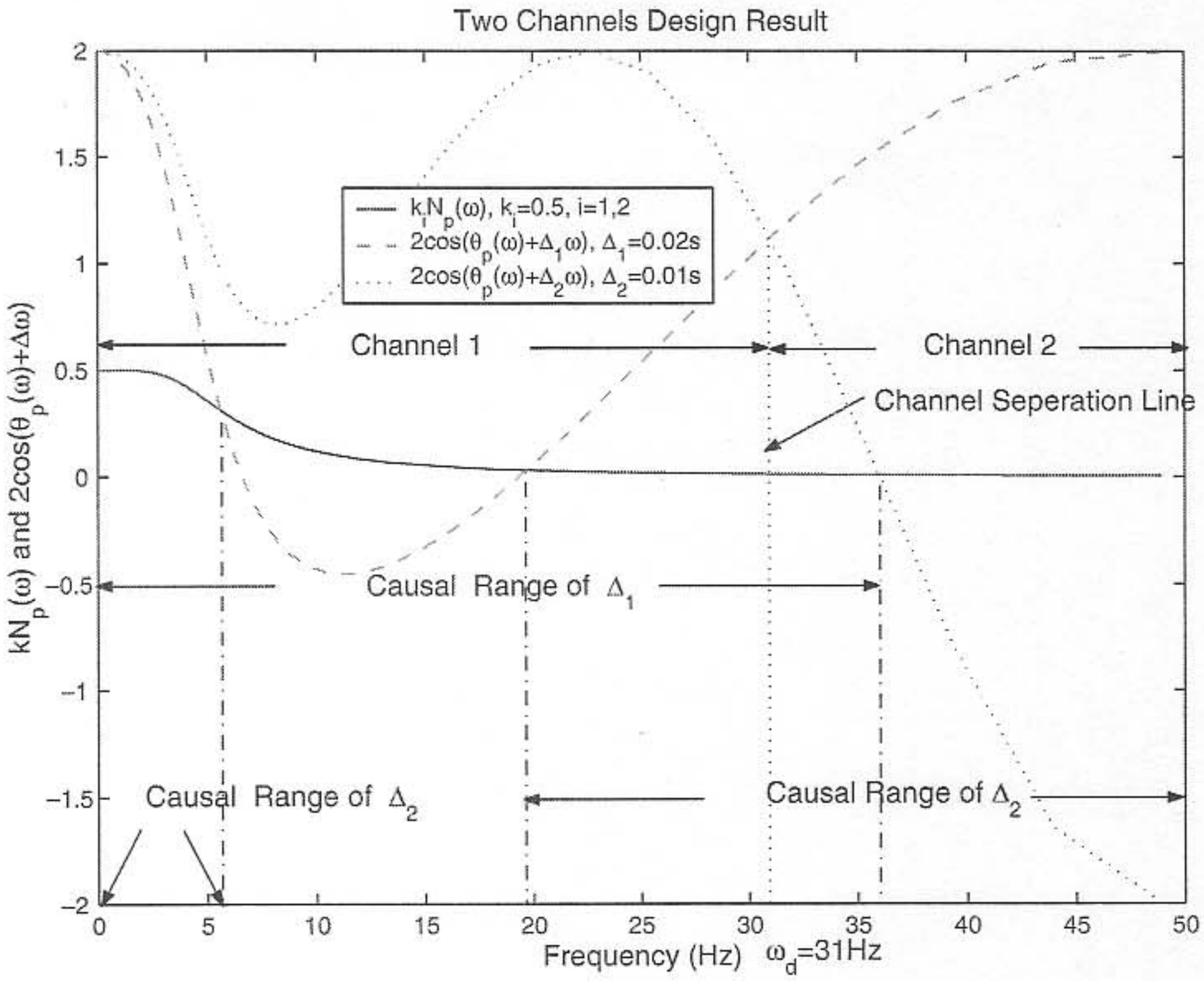


Figure 8. Design of two learning channels.

approach, a 28 Hz lowpass fifth-order Butterworth filter (The MathWorks Inc 1997) and a 33 Hz highpass fifth-order Butterworth filter are designed. The filters' design results are shown in figure 9. Note that the overlapping region of the two filters, [23, 36] Hz, is within [20, 36] Hz and conditions (10) and (11) are all satisfied. The two-channel learning are clearly effective as shown by the RMS error histories in the solid dashed lines in figure 10. RMS error continues decreasing after 200 repetitions. For comparison, single-channel A-type learning law is also performed. Learning gain $k=0.5$ is used and the cutoff frequency is 31 Hz, lower than the highest allowable cutoff frequency 36 Hz for robustness. Cutoff is realized by DFT/IDFT. The reason of letting the cutoff frequency coincide with the channel separation point is to clearly compare the learning effects of single-channel learning and multi-channel learning. The RMS error history of learning is shown in figure 10 with the dash-dot line. Learning convergence but RMS error stops decreasing after about 80 repetitions. This is because the single-channel A-type learns only the frequency components in the range [0, 31] Hz, compared with the wider learnable frequency band, [0, 50] Hz, of the proposed multi-channel learning scheme. For further comparison and to show the learning control effect of channel 2, the single-channel A-type learning law is also implemented without cutoff. The RMS error history of learning is shown in figure 10 with the dot line. RMS error exhibits a very slow increase after about 100 repetitions.

More insights can be observed by further examination of two error energies of channels 1 and 2, i.e. low frequency error energy inside [0, 31] Hz, in figure 11, and high frequency error energy inside [31, 50] Hz, in figure 12 (energy means the sum of power spectral density divided by length of power spectral density (The MathsWorks Inc.)). Figure 11 shows the low-frequency error energy histories in four cases. The low-frequency error energies in four cases decrease. The exception is that the single-channel A-type learning without cutoff seems starting diverging after 140 repetition. This may be due to the spillover effect of the divergence of the high frequency error components. Figure 12 shows the high frequency error energy histories in four cases. The high frequency error energies in the two multi-channel cases keep decreasing because the learning convergence is ensured by the A-type learning law in channel 2. In contrast, the high frequency error energy in the single channel without the cutoff case diverges slowly because condition (15) is violated at $\omega > 36$ Hz as shown in Figure 8. Eventually the slow increase of error will saturate the hardware limitation and may cause a digital

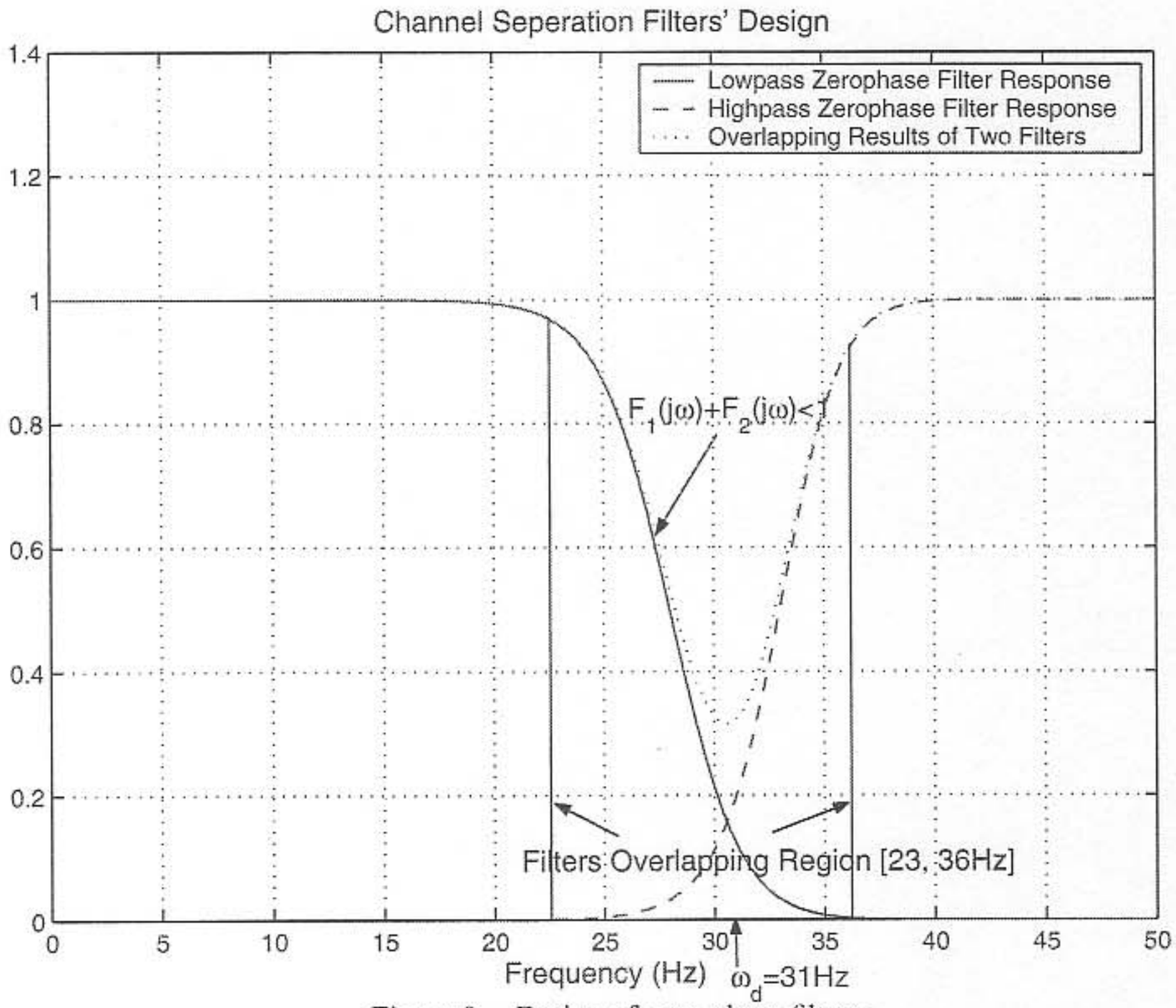


Figure 9. Design of zero-phase filters.

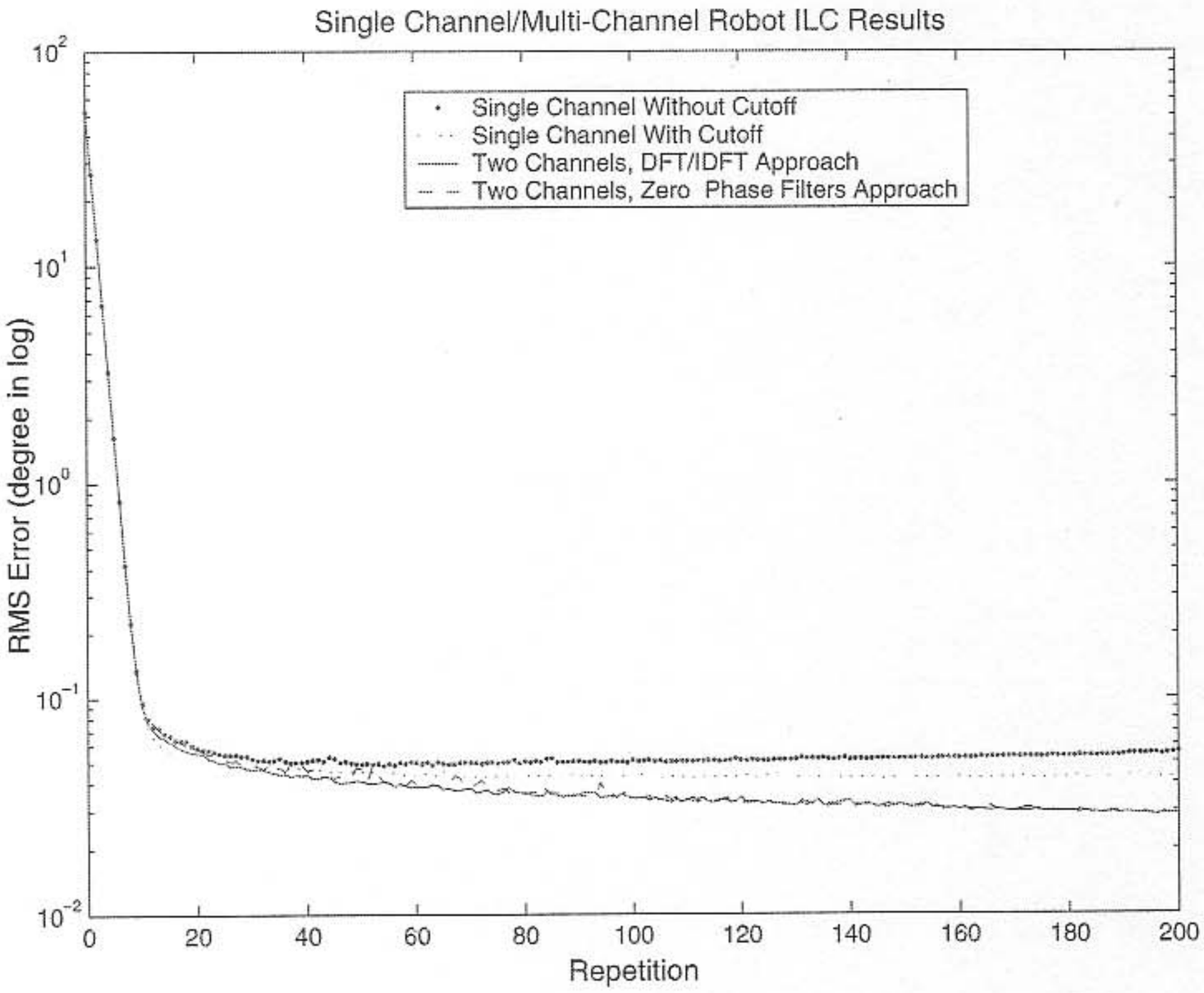


Figure 10. RMS error histories of 1 channel/2 channels.

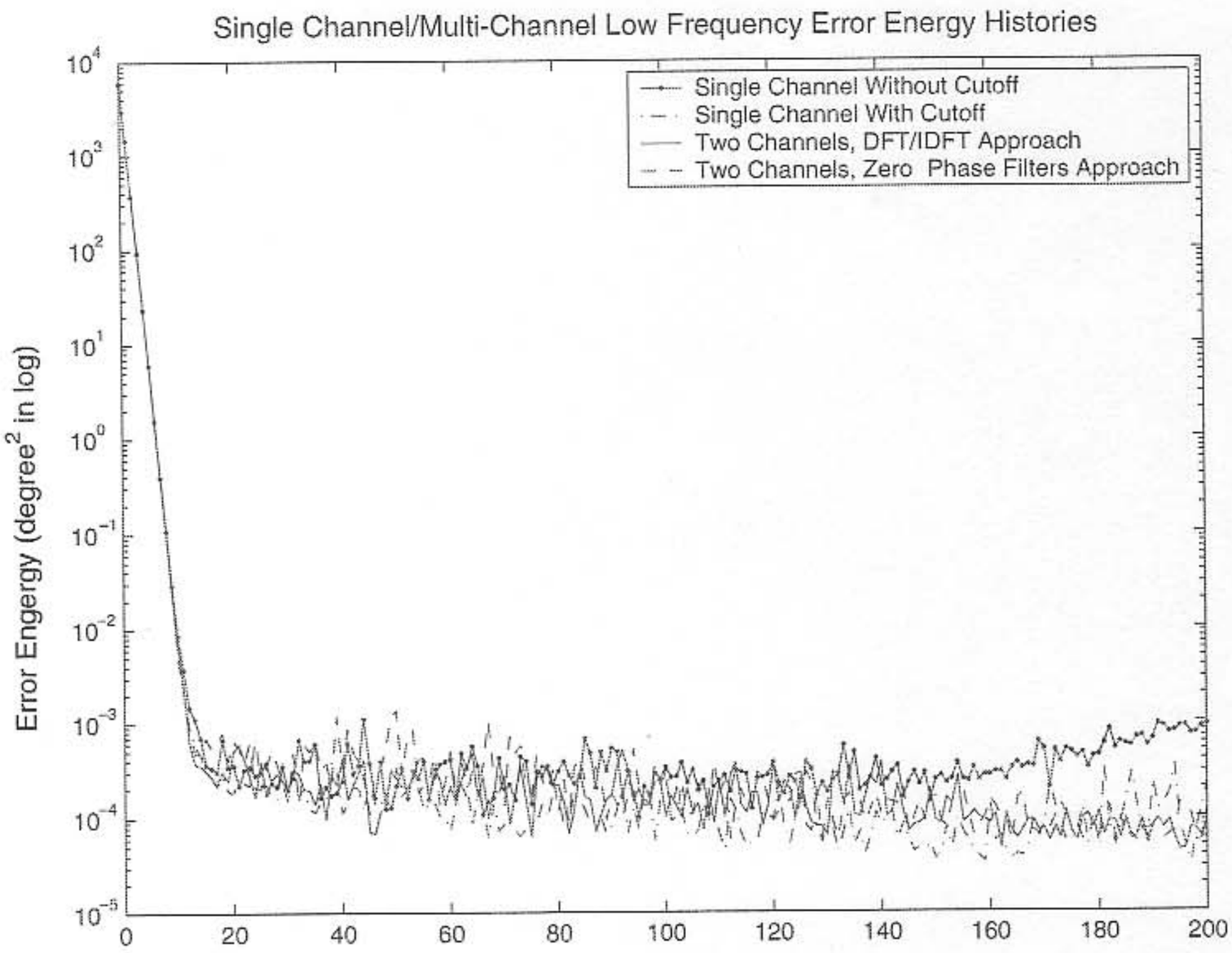


Figure 11. Low frequency error energy histories.

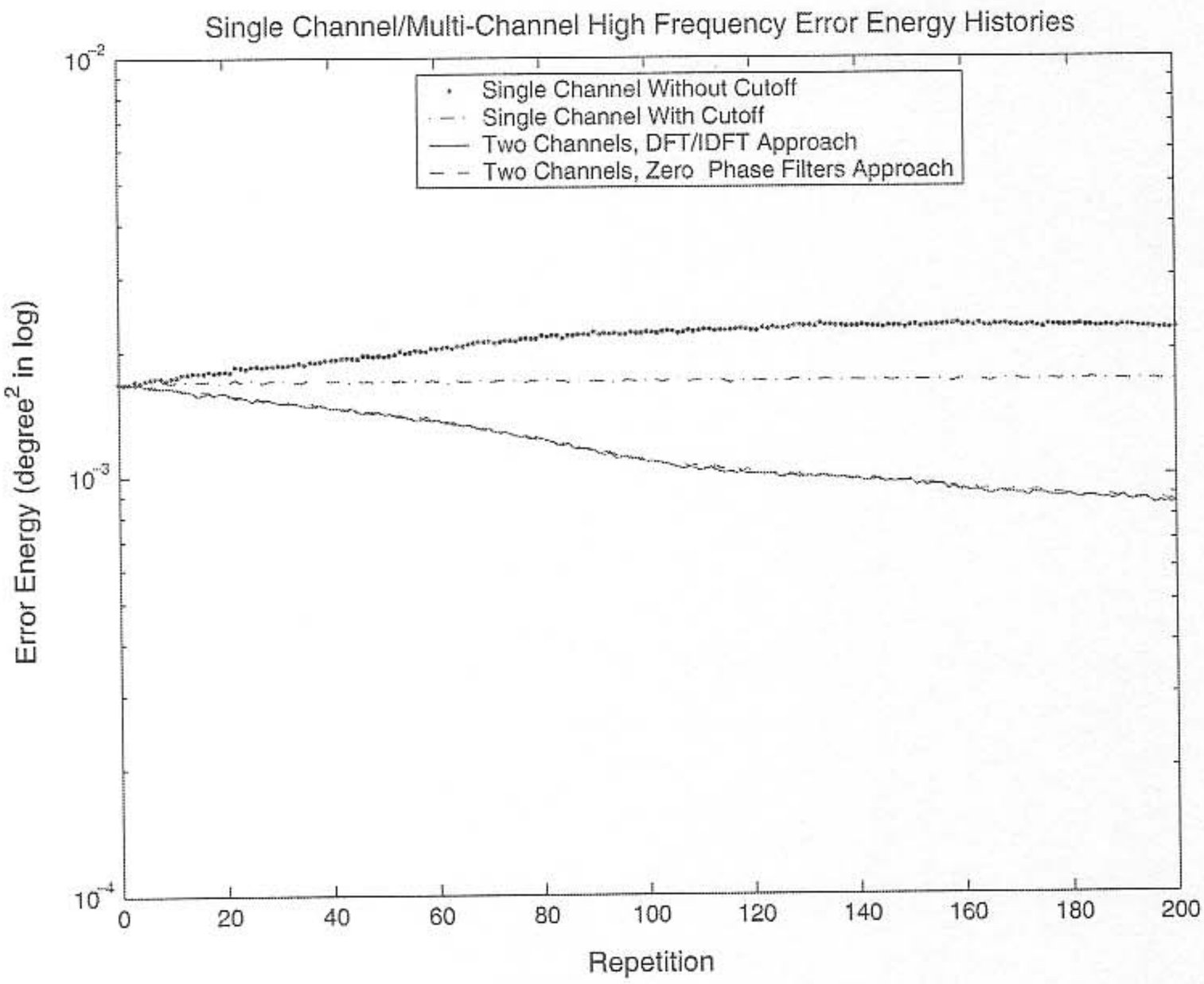


Figure 12. High frequency error energy histories.

overflow. This is referred to as long-term stability problem of ILC in Longman (2000). Finally, the case of single-channel with cutoff just leaves the high frequency error components inside channel 2 unaltered. Comparisons verify the working of the A-type learning controller in channel 2 in multi-channel learning.

## 7. Conclusion

The limited learnable frequency bandwidth achievable by a single iterative learning controller hampers the learning quality and final tracking accuracy. The multi-channels learning scheme proposed in this paper is able to overcome this limitation. The effectiveness and design of the multi-channel learning control is shown in widening the learnable frequency range. Multi-channel structure with more A-type learning laws is shown to outperform a single A-type learning control by both simulations and experiments. Wider learnable frequency range ensures better tracking performance. The multi-channel method can also apply to repetitive control using the batch update or real-time filtering techniques.

For comparison, we can approach the learnable bandwidth extension problem using sophisticated ILC laws. One such example is that an ILC designer can first work hard on system identification to get an accurate model, and then uses the inverse model based ILC. However, the advantages offered by ILC include the tolarence of inaccurate models and the simplicity of learning laws. The combination of the simple A-type law and the proposed multi-channel configuration does not rely on an accurate model and suits ILC design well. Furthermore, because the multi-channel learning controller uses only a few parameters, we should be able to use auto-tuning ideas to tune these parameters, such as lead-time $\Delta_i$, learning gain $k_i$, and channel separation point $\omega_d$ on the fly. Auto-tuning based multi-channel A-type ILC may reduce the reliance on a model or even do away with a model by tuning on-line.

## Acknowledgement

Part of the experimental results was presented at the 7th International Conference on Control, Automation, Robotics and Vision, Singapore, 2002.

## References

Amann, N., Owens, D. H., Rogers E., and Wahl, A., 1996, An $H_\infty$ approach to iterative learning control design. *International Journal of Adaptive Control and Signal Processing*, **10**, 767–781.

Arimoto, S., Kawamura, S., and Miyazaki, F., 1984, Bettering operation of robots by learning. *Journal of Robotic System*, **1**, 123–140.

Chen, Y.-Q., and Moore, K. L., 2001, On $D^\alpha$-type iterative learning control, in *Proceedings of the 40th IEEE Conference on Decision and Control*, Orlando, FL USA, pp. 4451–4456.

Doh,T.-Y., Jin, K. B., and Chung, M. J., 1998, An LMI approach to iterative learning control for uncertain linear systems. In *Proceedings of the World Automation Congress (WAC)*, Anchorage, AL, USA, pp. ISIAC006.1–6.

Goh, C. J., 1994, A frequency domain analysis of learning control. *Journal of Dynamic Systems, Measurement, and Control*, **116**, 781–786.

Hideg, L. M., and Judd, R. P., 1988, Frequency domain analysis of learning systems, *Proceedings of the 27th Conference on Decision and Control*, Austin, TX, USA, pp. 586–591.

Huang, W., and Cai, L., 2000, New hybrid controller for systems with deterministic uncertainties, *IEEE/ASME Transactions on Mechatronics*, **5**, pp. 342–348.

Lee, J.-W., Lee, H.-S., and Bien, Z., 1993, Iterative learning control with feedback using Fourier series with application to robot trajectory tracking, *Robotic*, **11**, 291–298.

Les, T., 1996, *Analog and Digital Filter Design Using C*. Upper Saddle River, NJ: Prentice-Hall PTR.

Longman, R. W., 2000, Iterative learning control and repetitive control for engineering practice. *International Journal of Control*, **73**, 930–954.

Longman, R. W., and Songchon, T., 1999, Trade-offs in designing learning/repetitive controller using zero-phase filter for long term stabilization, *Advances in the Astronautical Sciences*, **102**, 673–692.

Longman, R. W., and Wirkander, S.-L., 1998, Automated tuning concepts for iterative learning and repetitive control laws. *Proceeding of the 37th IEEE Conference on Decision and Control*, Tampa, FL, USA, pp. 192–198.

Manabe, T., and Miyazaki, F., 1991, Learning control based on local linearization by using DFT, *Proceedings of the 1991 IEEE/RSJ International Workshop on Intelligent Robots and Systems*, Osaka, Japan, pp. 639–646.

Moon, J.-H., Doh T.-Y., and Chung, M. J., 1998, A robust approach to iterative learning control design for uncertain systems, *Automatica*, **34**, 1001–1004.

Phan, M., and Juang, J., 1996, Design of learning controllers based on an auto-regressive representation of a linear system, *AIAA Journal of Guidance, Control and Dynamics*, **19**, 355–362.

Plotnik, A. M., and Longman, R. W., 1999, Subtitles in the use of zero-phase low-pass filtering and cliff filtering in learning control. *Advances in the Astronautical Sciences*, **103**, 673–692.

Tayebi, A., and Zaremba, M. B., 2002, Iterative learning control for non-linear systems described by a blended multiple model representation. *International Journal of control*, **75**, 1376–1383.

Tan, K. K., Dou, H. F., Chen, Y. Q., and Lee, T. H., 2001, High precision linear motor control via relay-tuning and iterative learning based on zero-phase filtering. *IEEE Transaction on Control System Technology*, **9**, 244–253.

Wang, D., 2000, On D-type and P-type ILC designs and anticipatory approach. *International Journal of Control*, **73**, 890–901.

Wirkander, S.-L., and Longman, R. W., 1999, Limit cycles for improved performance in self-tuning learning control. *Advances in the Astronautical Sciences*, **102**, pp. 763–781.

Ye, Y., and Wang, D., 2002, Multi-channel design for ILC with robot experiments. *Proceedings of the Seventh International Conference on Control, Automation, Robotics and Vision (ICARCV2002)*, Singapore, pp. 1066–1070.

The Maths Works, Inc., 1997, *Signal Processing Toolbox User's Guide*.